OncoTargets and Therapy

Dovepress
Taylor & Francis Group

Open Access Full Text Article

ORIGINAL RESEARCH

Multi-cohort Validation Based on Disulfidptosis-Related lncRNAs for Predicting Prognosis and Immunotherapy Response of Esophageal Squamous Cell Carcinoma

Zhongquan Yi[1,*], Xia Li[2,*], Yangyang Li[3,*], Yanan Ji[1], Jing Zhao[1], Heling Xu[4], Lei Zhou[5], JianXiang Song[3]

[1]Department of Central Laboratory, Affiliated Hospital 6 of Nantong University, Yancheng Third People's Hospital, Yancheng, Jiangsu, 224000, People's Republic of China; [2]Department of General Medicine, Affiliated Hospital 6 of Nantong University, Yancheng Third People's Hospital, Yancheng, Jiangsu, 224000, People's Republic of China; [3]Department of Cardiothoracic Surgery, Affiliated Hospital 6 of Nantong University, Yancheng Third People's Hospital, Yancheng, Jiangsu, 224000, People's Republic of China; [4]Department of Gastroenterology, Affiliated Hospital 6 of Nantong University, Yancheng Third People's Hospital, Yancheng, Jiangsu, 224000, People's Republic of China; [5]Department of General Surgery, Affiliated Hospital 6 of Nantong University, Yancheng Third People's Hospital, Yancheng, Jiangsu, 224000, People's Republic of China

*These authors contributed equally to this work

Correspondence: Lei Zhou; JianXiang Song, Email zhoulei@ntu.edu.cn; jxsongycsy@163.com

Background: Disulfidptosis, a novel pattern of regulatory cell death, provides a valuable opportunity to gain deeper comprehension of tumor pathogenesis and treatment strategies. However, its biological mechanism in esophageal squamous cell carcinoma (ESCC) has yet to be completely elucidated.

Materials and Methods: From the Gene Expression Omnibus (GEO) GSE53625 dataset, we obtained RNA-seq data and clinical information. An analysis of Pearson correlation was utilized to screen disulfidptosis-related lncRNAs (DRLs), followed by LASSO and multivariate Cox regression analysis to construct a prognostic signature. The reliability and accuracy of this signature were verified on internal validation sets, including training (n= 90), testing (n= 89), and GSE53625 entire (n= 179) sets, as well as external sets, including TCGA-ESCC (n= 81) and GSE53624 (n= 119) sets. Additionally, mutation data comes from TCGA database was utilized for validating tumor mutation burden (TMB) analysis. In cell lines, an analysis of lncRNA differential expression was conducted using qRT-PCR.

Results: Ultimately, six DRLs were utilized to construct a prognostic signature. Across all sets, Kaplan–Meier analysis indicated that high-risk ESCC patients have a poorer prognosis ($p < 0.05$), and ROC analysis showed that the AUC values at 1, 3, and 5 years all exceeded 0.6. Moreover, disparities were observed in immune phenotype scores, tumor infiltration of immune cells, functional enrichment, TIDE score, immune function, and TMB among the two risk groups. Additionally, individuals at high risk showed higher sensitivity to erlotinib, acetalax, gefitinib, lapatinib, sapitinib, and afatinib.

Conclusion: Through bioinformatics analysis, a novel and robust DRLs signature for ESCC was established, providing new insights into the prognosis prediction and potential treatment strategies. Nevertheless, this study is retrospective and relies on public databases, with a limited sample size within the datasets. In the future, it is essential to conduct more extensive validation of the prognostic value and efficacy in real ESCC cohorts.

Keywords: esophageal squamous cell carcinoma, disulfidptosis, lncRNA, prognosis, immunotherapy

Introduction

Esophageal squamous cell carcinoma (ESCC) is the predominant type of esophageal cancer, accounting for over 3% of global cancer incidence.[1–3] Although treatment for ESCC is improving, the 5-year postoperative survival rate remains low.[4] Besides, since ESCC is typically diagnosed at an advanced stage or metastatic, there are few treatment options

Received: 12 February 2025
Accepted: 22 June 2025
Published: 25 June 2025

available.[5] Furthermore, due to treatment resistance and recurrence, the prognosis of ESCC patients remains poor.[6–8] Consequently, the investigation of innovative and robust prognostic prediction models is critical for early ESCC diagnosis and developing effective treatment strategies, ultimately improving the prognosis of ESCC patients.

Recently, a new type of regulatory cell death known as disulfidptosis was discovered. Disulfidptosis is triggered by the abnormal accumulation of intracellular disulfides during glucose starvation, ultimately leading to cell death from disulfide stress.[9] It should be emphasized that disulfidptosis is distinct from the previously identified forms of cell death.[9–11] Some recent studies have found potential links between disulfidptosis and cancer through bioinformatics analysis.[11–19] For example, in clear cell renal cell carcinoma, Yang et al found that the disulfidptosis-related gene AJAP1 could potentially serve as a biomarker.[11] In bladder cancer, Zhao et al constructed a signature related to disulfidptosis and evaluated its value in survival prediction, tumor microenvironment (TME), and immunotherapy responses.[12] Additionally, in hepatocellular carcinoma, Xu et al built a disulfidptosis-related lncRNAs (DRLs) signature and found it to be a dependable indicator of prognosis and treatment response.[18]

Researchers have uncovered a significant correlation between lncRNA, a noncoding RNA spanning at least 200 nucleotides,[20] and the development and progression of ESCC.[21–24] For instance, the advancement of ESCC was facilitated by LncRNA LUESCC through targeting the miR-6785-5p/NRSN2 axis.[24] Similarly, Zhao et al noted that LINC00330 inhibited ESCC progression by blocking CCL2 mediated tumor associated macrophages reprogramming.[23] Moreover, many studies indicates that constructing lncRNA signatures is valuable for predicting ESCC patient prognosis and provides new clinical insights for targeted therapies.[21,25,26] For instance, in ESCC, Zhang et al showed that a cuproptosis-related five-lncRNA signal effectively predicts prognosis and guides immunotherapy and chemotherapy.[25]

In recent studies, it has been discovered that the prognostic signatures utilizing DRLs hold substantial significance in predicting the prognosis of cancer patients and their responses to immunotherapy.[16,17,27–36] For instance, in bladder cancer, Han et al,[27] Hu et al,[28] and Xiao et al[29] respectively established the DRLs signatures and demonstrated that they were reliable prognostic indicators for patients. In laryngeal squamous cell carcinoma, Zhang et al[31] developed a DRLs signature and found it was capable of predicting both prognosis and therapeutic responses in patients. Regarding liver hepatocellular carcinoma, Liu et al[17] constructed a DRLs signature and assessed its significance in prognostic prediction, TME, and immunotherapy responses. However, the potential of DRLs signature in predicting the prognosis of ESCC remains uninvestigated. Additionally, its capacity to forecast the immunotherapy response of ESCC has not been explored thus far. Consequently, further research into the impact of the DRLs signature on ESCC is imperative.

In this study, we employed a variety of bioinformatics approaches to construct a DRLs signature for assessing the prognosis, TME, and the efficacy of immunotherapy response in patients with ESCC, as well as sensitivity to antitumor agents. This study aims to clarify the function of DRLs signatures in ESCC, providing new insights for the prognosis prediction and potential treatment strategies of ESCC patients.

Materials and Methods

Data Processing

The general study process is illustrated in Figure 1. Based on current research,[9] 16 disulfidptosis-related genes (DRGs) were excerpted. We obtained the RNA-seq data from the Gene Expression Omnibus (GEO) and The Cancer Genome Atlas (TCGA) database. This research incorporates three published sets: GSE53625 (n = 179), GSE53624 (n = 119), and TCGA-ESCC (n = 81). The GSE53625 set was split into training (90 patients) and testing sets (89 patients) using the R package "caret" in a random manner, maintaining an approximate 1:1 ratio. Table 1 displays the baseline characteristics of both the training and testing sets, showing no significant disparities. The prognostic signature of ESCC was externally validated using GSE53624 and TCGA-ESCC sets.

Development and Validation of the Signature

From the GSE53625 set, we obtained LncRNA expression pattern data. Using Pearson correlation analysis, we examined the relationship between lncRNAs and 16 DRGs. Specifically, DRLs were identified when their Pearson ($R > 0.4$ and $p < 0.01$). The GSE53625 training set was used to establish the DRLs signature, while the GSE53625 testing set, GSE53625 entire set,

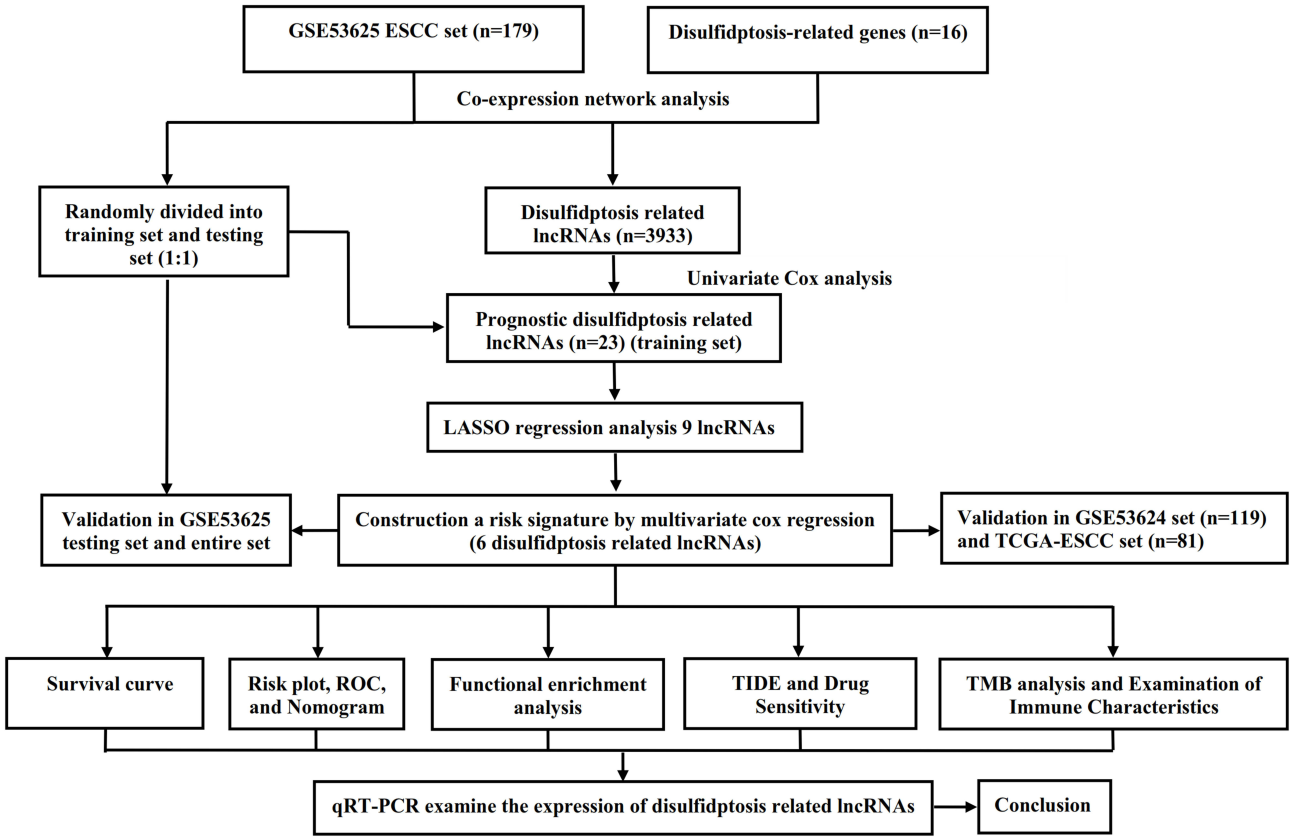

Figure 1 The flow chart of research design.
Abbreviations: ESCC, esophageal squamous cell carcinoma; LASSO, Least Absolute Shrinkage and Selection Operator; ROC, receiver operating characteristic; TIDE, tumor immune dysfunction and exclusion; TMB, tumor mutational burden.

GSE53624 set, and TCGA-ESCC set were used to verify the signature. The endpoint of the study was overall survival (OS). Prognostic DRLs were determined utilizing univariate Cox regression analysis ($p < 0.05$). Then, the study employed LASSO regression to identify relevant prognostic lncRNAs. Through a stepwise regression approach, we were able to construct the

Table 1 Comparisons of Patient Characteristics Between Training and Testing Sets

Characteristics	Total Set (n = 179)	Training Set (n = 90)	Testing Set (n = 89)	*P*-value
Age				
≤60	99 (55.31%)	47 (52.22%)	52 (58.43%)	0.404
> 60	80 (44.69%)	43 (47.78%)	37 (41.57%)	
Gender				
Male	146 (81.56%)	69 (76.67%)	77 (86.52%)	0.089
Female	33 (18.44%)	21 (23.33%)	12 (13.48%)	
T stage				
T1	12 (6.71%)	3 (3.33%)	9 (10.11%)	0.546
T2	27 (15.08%)	20 (22.22%)	7 (7.87%)	
T3	110 (61.45%)	53 (58.89%)	57 (64.04%)	
T4	30 (16.76%)	14 (15.56%)	16 (17.98%)	
N stage				
N0	83 (46.37%)	41 (45.56%)	42 (47.19%)	0.826
N1, N2, N3	96 (53.63%)	49 (54.44%)	47 (52.81%)	
TNM stage				
I	10 (5.59%)	5 (5.56%)	5 (5.62%)	0.996
II	77 (43.02%)	39 (43.33%)	38 (42.7%)	
III	92 (51.39%)	46 (51.11%)	46 (51.68%)	

https://doi.org/10.2147/OTT.S519270

most effective prognostic signature using multivariate cox regression analysis. The risk score for each patient was calculated utilizing the following formula: Risk score =∑i = EXP(i)× LnCoef(i). In accordance with the median risk score, each ESCC patient was categorized as either high-risk or low-risk. Next, to evaluate the ability of this signature in predicting ESCC prognosis, we conducted Kaplan-Meier (KM) and Receiver operating characteristic (ROC) analysis to examine its effectiveness and accuracy.[37]

Clinical Characteristics of the DRLs Signature and Constructing a Nomogram Plot

To validate the applicability of the DRLs signature to subgroups of patients with diverse clinical characteristics, patients with ESCC were stratified into distinct clusters according to their age, gender, positive lymph node (N), tumor (T), and stage. Subsequently, based on the median riskscore of patients in different clusters, ESCC patients were classified into high- and low-risk groups. KM analysis was employed to assess the accuracy of the DRLs signature in predicting the prognosis of different patient subgroups.

Taking into account various ESCC patients' clinical feature (including age, T, gender, N, and stage), univariate and multivariate Cox regression analyses were conducted to investigate whether the DRLs signature could serve as a standalone risk factor ($p < 0.05$). Additionally, a nomogram was constructed using the "rms" package to estimate the 1-, 3-, and 5-year OS rates of patients with ESCC.[38] Calibration curves were also utilized to compare predicted values with actual observations, and consistency index (C index) and decision curve analysis (DCA) were utilized to analyze the predictive ability.

Functional Enrichment Analysis

Utilizing the "limma" package, differentially expressed genes (DEGs) between risk groups were identified ($|logFC| > 0.5$ and $p < 0.05$).[39] Relevant analyses were implemented through "clusterProfiler" R package[40] to examine the potential function of DEGs. These analyses included Gene Ontology (GO, which encompasses biological process (BP), cellular component (CC), and molecular function (MF)) and Kyoto Encyclopedia of Genes and Genomes (KEGG) analyses. Additionally, to evaluate potential pathways for signaling and biological functional alterations between groups, Gene Set Enrichment Analysis (GSEA) were applied by utilizing KEGG and Hallmark gene sets ($p < 0.05$).

Analysis of Immune Cell Infiltration, Tumor Immune Dysfunction and Exclusion (TIDE), Tumor Mutational Burden (TMB), and Drug Sensitivity

The ESTIMATE method was utilized to calculate the estimate and immune scores for each ESCC sample, as well as the stromal score. Besides, the abundance of 22 immune cells infiltration between risk groups was assessed through CIBERSORT method.[41] Additional, the overall immune function in patients with ESCC were assessed via single sample gene set enrichment analysis. To compare the distribution of immune cells and the disparities in overall immune function between the two risk groups, the Wilcoxon test was employed.

Furthermore, TIDE scores for each patient were acquired through the online website (http://tide.dfci.harvard.edu/).[42] The correlation between the TIDE score and risk score was examined via Pearson correlation analysis. Moreover, the Wilcoxon test and Chi-square test were employed to compare the differences in the TIDE score and immunotherapy response between the high- and low-risk groups.

Herein, utilizing the "maftools" package, we analyzed the TMB data downloaded from TCGA database.[43] The correlation between riskscore and TMB was evaluated via Pearson analysis. Additionally, the variances in TMB between distinct risk level groups were compared using the Wilcoxon test.

Utilizing the "oncoPredict" package,[44] we initiated drug sensitivity analysis to identify potential antitumor agents. Pearson correlation analysis was used to analyze the association between half-maximal inhibitory concentration (IC50) values and the risk scores of various drugs, and the Wilcoxon test was used to compare the drug sensitivity scores between different risk groups.

Cell Culture and qRT-PCR

Two ESCC cells (KYSE30 and KYSE150) were obtained from Priscilla (Wuhan, China), and cultured in Roswell Park Memorial Institute-1640 (RPMI-1640; Priscilla) supplemented with 10% fetal bovine serum (FBS; Priscilla) and 100 μg/mL penicillin-streptomycin (Priscilla). The Het-1A normal esophageal epithelial cells were sourced from the Chinese Academy of Sciences Cell Bank (Shanghai, China) and cultured in Dulbecco Modified Eagle Medium (DMEM; Priscilla) with 10% FBS and 100 μg/mL penicillin-streptomycin. These cells were cultured at 37°C in a humidified incubator at 5% CO2.

Total RNA was extracted from cell lines utilizing the TRIzol reagent (Thermo Scientific, USA). ChamQ SYBR qPCR Master Mix (Vazyme, China) was used for conducting qRT-PCR, with GAPDH being utilized as the endogenous control for normalizing target gene expression. The primer sequences for determining relative gene expression are listed in Table 2.

Statistical Analysis

To conduct the statistical analyses, GraphPad and R 4.3.1 were used. According to the specific circumstances, we employed either the Student's *t*-test or Wilcoxon rank sum test for intergroup comparisons. Pearson correlation coefficient was utilized to assess correlation between variables. Chi-square test was implemented to evaluate whether there are differences in clinical characteristics. All statistical tests were considered significant at $p < 0.05$.

Results

Identification and Construction of DRLs Signature

According to Pearson correlation analysis, 3933 LncRNAs were screened and significantly correlated with at least one of the 16 DRGs (Figure 2A). Through univariate Cox regression analysis, 23 prognostic LncRNAs were selected ($p < 0.05$) in the training set (Figure 2D). Among these, eight LncRNAs were categorized as "risk" genes, while the rest of LncRNAs were categorized as "protective" genes. Subsequent LASSO regression analysis identified a minimum lambda value of 9 (Figure 2B and C). After multivariate Cox regression screening, a risk signature was developed based on six LncRNAs (Figure 2E) (AL359706.1, AC025774.1, AC011840.1, AC021683.3, AC079768.3, and AL121904.1). Following formula: Risk score = AL359706.1* 1.02224 + AC025774.1 * 0.36626 + AC011840.1 * (−0.17434) + AC021683.3 * (−0.53773) + AC079768.3 * (−0.36812) + AL121904.1 * (−0.49455), each ESCC patient's risk score was computed. The correlation heatmap depicted the relative correlation coefficients between these 6 LncRNAs and 16 DRGs (Figure 2F).

Table 2 Primer Sequences for qRT-PCR

Primer name	Primer Sequence
AL359706.1	F: CCAGGAGAGCCAATTTCTGAC
	R: GGAGGTAAGCTGAAGTCTGTGA
AC025774.1	F: CCGGTGGGACACAAATCCAA
	R: CTTCCCATGGCAAAATGCACA
AC011840.1	F: GCTGGCCACTCAGTATTCCTTGTC
	R: CCAACCTGGACTTCCTCCGTGA
AC079768.3	F: CTTTCTTCTGTCTTCAGCTTGTACC
	R: GATTCCTTCATGTCATCCTCATAACG
AL121904.1	F: GGCAGAATACAAAAAGGTGTCACAG
	R: TCATCTCCAGCTAGTGCATTTCCAT
AC021683.3	F: CTGGCACTCATGGGTCTATGGA
	R: ATCTGCAGCCACTTTGATGTTG
GAPDH	F: GGAGCGAGATCCCTCCAAAAT
	R: GGCTGTTGTCATACTTCTCATGG

https://doi.org/10.2147/OTT.S519270

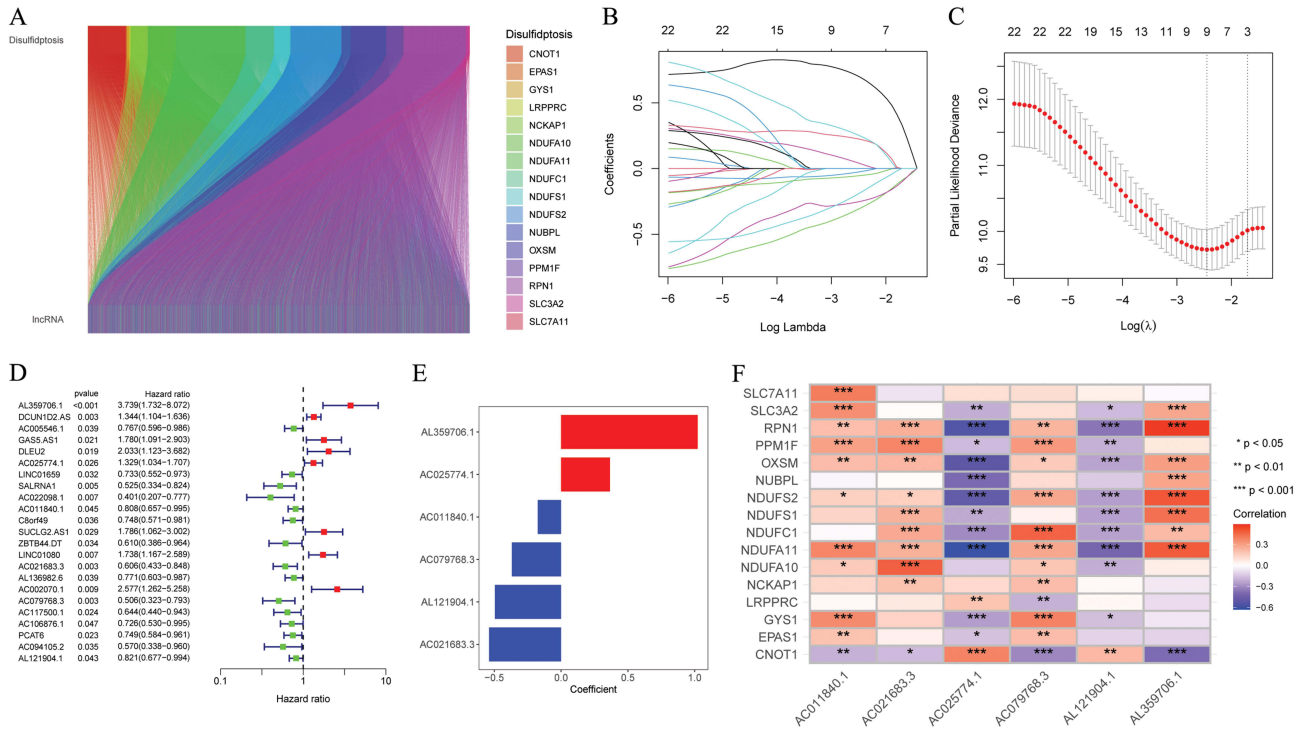

Figure 2 Identification and construction of DRLs signature. (**A**) Sankey relation diagram for disulfidptosis-related genes and lncRNAs. (**B** and **C**) The coefficient profile of prognostic lncRNAs by LASSO regression analysis. (**D**) Forest plot of prognostic LncRNAs. (**E**) Multivariate Cox coefficients for 6 lncRNAs in the prognostic signature. (**F**) Heatmap showing the correlation between the 6 lncRNAs involved in the prognostic signature and 16 disulfidptosis-related genes.
Note: *$p < 0.05$, **$p < 0.01$, ***$p < 0.001$.
Abbreviations: DRLs, disulfidptosis-related lncRNAs; LASSO, Least Absolute Shrinkage and Selection Operator.

Prognosis Prediction of ESCC Patients Utilizing the DRLs Signature

In accordance with the median score of training set, each ESCC patient was classified as either the high-risk or low-risk within their respective sets for training, testing, and GSE53625, respectively. The heatmap of six DRLs expression and the distribution of OS status and risk score were presented in Figure 3B–D. After conducting KM analysis, it was observed that low-risk ESCC group showed better OS compared to high-risk ESCC group across all sets ($p < 0.05$) (Figure 3A). Following internal validation, GSE53624 and TCAG-ESCC were selected as external sets to reconfirm the predictive effects of the signature. According to the results, both external validation and internal validation sets exhibit good cross-validation effects (Figure 3E and F). ROC analysis showed that the AUC values at 1, 3, and 5 years all exceeded 0.6 in both the internal and external sets (Figure 3G–I).

Clinical Prognostic Analysis

Among ESCC patients in GSE53625 set, age was categorized into > 60 years and ≤ 60 years; Gender was categorized into male and female; T was categorized into T1-T2 and T3-T4; N was categorized into N0 and N1-3; overall stage was categorized into I–II and III. As shown in Figure 4A–J, across all subgroups, the low-risk ESCC group exhibited a higher survival rate than the high -risk ESCC group ($p < 0.05$).

Independent Prognosis of DRLs Signature

In GSE53625 set, as depicted in Figure 5A, age, N, stage, and risk score were identified as prognostic risk factors for ESCC patients through univariate regression Cox analysis ($p < 0.05$). Subsequently, multivariate Cox regression analysis revealed age ($p = 0.015$) and risk score ($p < 0.001$) as independent prognostic risk factors for ESCC patients. Furthermore, in the GSE53624 set (Figure 5B), we observed that risk score continued to be an independent prognostic risk factor ($p < 0.001$), indicating its robust prognostic ability in ESCC patients.

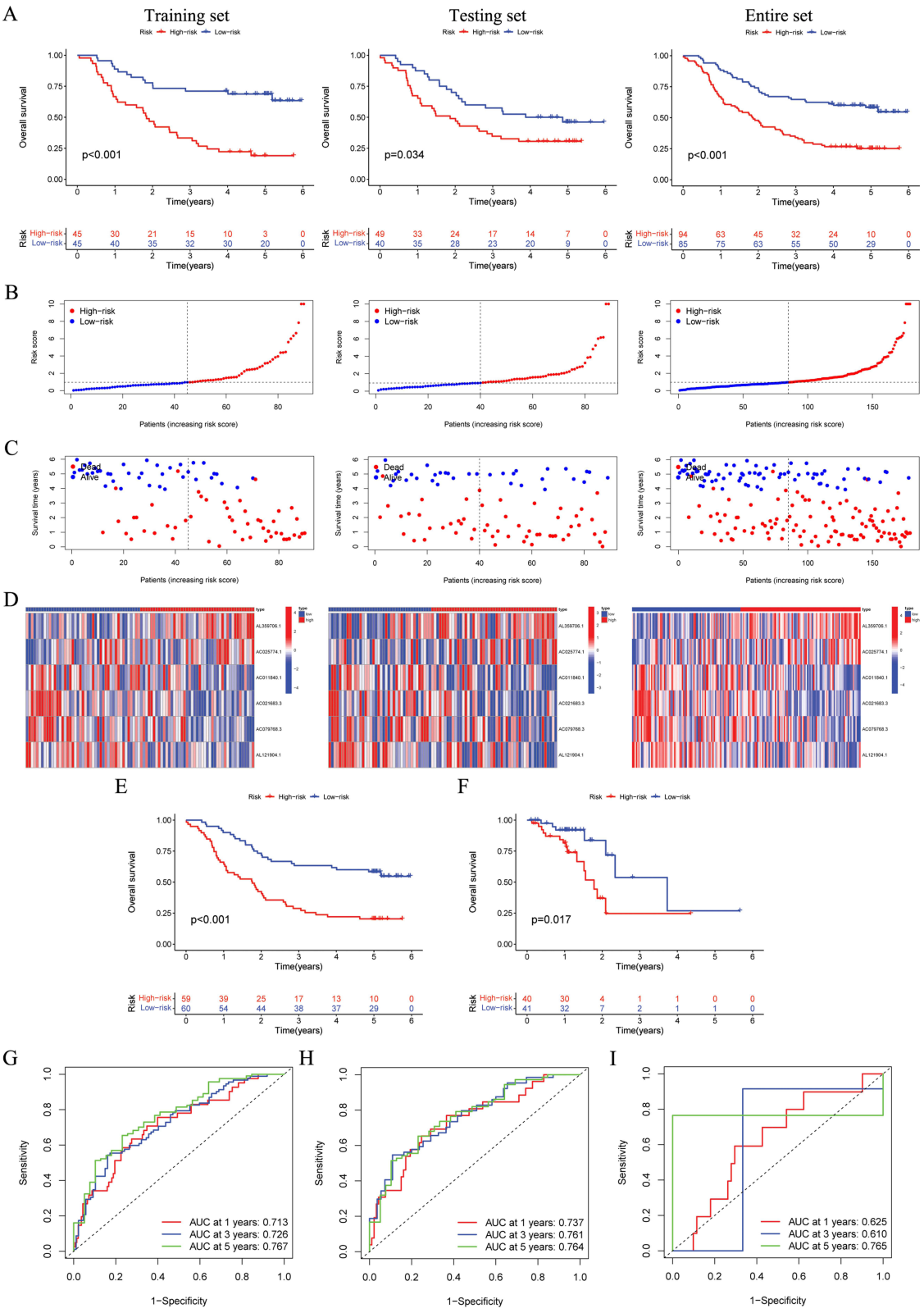

Figure 3 The validation of the prognostic signature in both internal and external sets. (**A**) OS of patients in different risk groups in the GSE53625 training, testing, and entire sets. (**B** and **C**) The distribution of risk score and overall survival status for each patient in the GSE53625 training, testing, and entire sets. (**D**) Heatmap showing the expression of six disulfidptosis-related lncRNAs in the GSE53625 training, testing, and entire sets. (**E**) OS of patients in different risk groups in the GSE53624 set. (**F**) OS of patients in different risk groups in the TCGA-ESCC set. (**G**–**I**) ROC curves for predicting 1-, 3- and 5-year OS in the GSE53625, GSE53624, and TCGA-ESCC sets.
Abbreviations: OS, overall survival; ROC, Receiver operating characteristic; ESCC, esophageal squamous cell carcinoma.

https://doi.org/10.2147/OTT.S519270

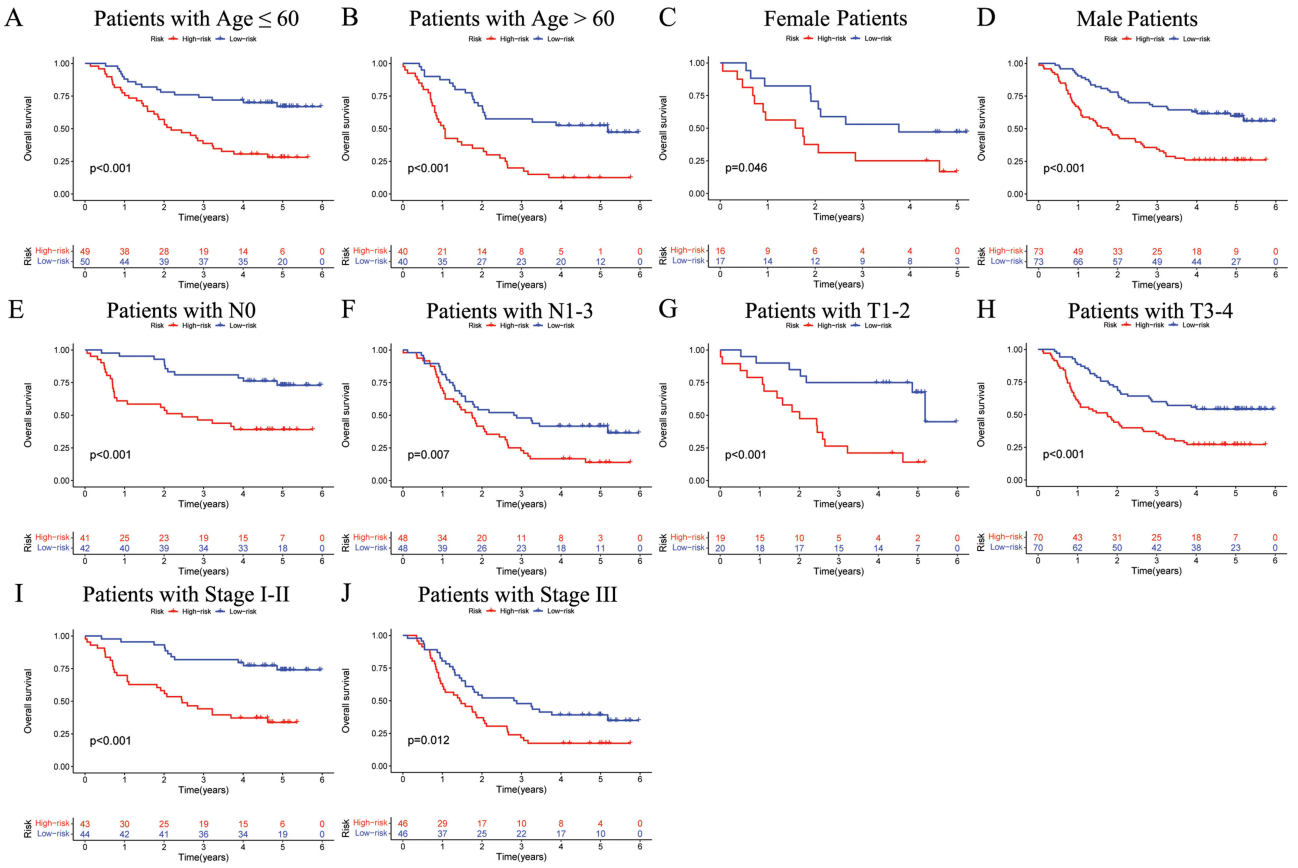

Figure 4 Kaplan–Meier analysis of OS in different subgroups based on the clinical features of patients with ESCC in the GSE53625 set. (**A**) Age ≤ 60 years. (**B**) Age > 60 years. (**C**) Female. (**D**) Male. (**E**) N0. (**F**) N1-3. (**G**) T1–T2. (**H**) T3–T4. (**I**) Stage I–II. (**J**) Stage III.
Abbreviations: OS, overall survival; ESCC, esophageal squamous cell carcinoma.

We developed a DRLs nomogram utilizing risk score and various clinical features (Figure 5C). ROC analysis revealed that nomogram exhibited a high level of specificity and sensitivity (Figure 5D). The calibration curve showed high consistency between the findings of the nomogram and the observed probability of OS in practical application (Figure 5E). The results from the C index and DCA indicated that the nomogram has a more robust and strong predictive capability as well as net clinical benefit than other clinical features (Figure 5F and G), indicating that this nomogram has the potential to be utilized as a precise prognostic tool for ESCC patients.

Different Tumor-Associated Pathways Between Groups

Supplementary Table 1 presents the genes exhibiting 855 DEGs between risk groups. DEGs significantly contributed to the "immune system process" within the BP category. In the field of CC, there was a notable enrichment in terms of "extracellular region", "extracellular space", and "endomembrane system". In the category of MF, DEGs exhibited notable enrichment in "signaling receptor binding", "molecular function regulator", and "receptor ligand activity" (Figure 6B). KEGG pathway analysis indicated that DEGs were predominantly associated with "Pentose and glucuronate interconversions", "Cytokine-cytokine receptor interaction", "Metabolism of xenobiotics by cytochrome P450", and "Neuroactive ligand-receptor interaction" (Figure 6A). Furthermore, the GSEA analysis indicated a notable difference between subgroups. The high-risk group primarily showed activation of various cancer-related and immune-related signaling pathways, such as JAK-STAT signaling, antigen processing and presentation, the intestinal immune network for IgA production, and TGF-β signaling pathway (Figure 6C and E). The low-risk group primarily exhibited activation of signaling pathways associated with tumor metabolic dysfunction, such as glutathione metabolism and the pentose and glucuronate interconversions (Figure 6D and F).

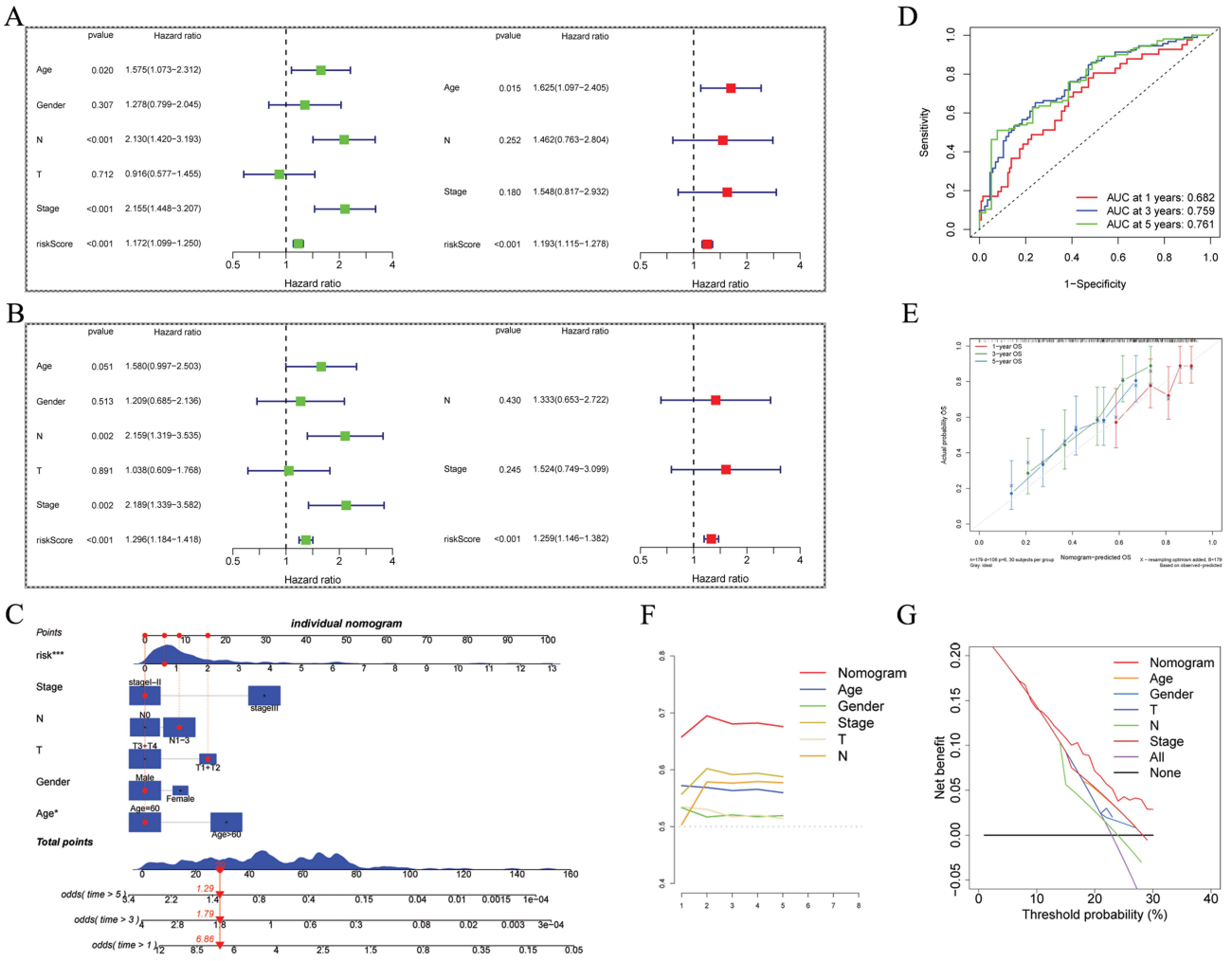

Figure 5 Independent prognostic analysis and construction of a nomogram. (**A**) Univariate and multivariate analyses of the clinical characteristics and risk score for the OS in the GSE53625 set. (**B**) Univariate and multivariate analyses of the clinical characteristics and risk score for the OS in the GSE53625 set. (**C**) Nomogram. (**D**) ROC curves showing the prediction performance of the nomogram in 1, 3, and 5-year OS. (**E**) Calibration curve of the nomogram for 1, 3, and 5-year OS. (**F**) The comparison of the C index between the nomogram and other clinical features. (**G**) Decision curve analysis showing the net benefit by applying the nomogram and other clinical features.
Note: *$p < 0.05$, ***$p < 0.001$.
Abbreviations: OS, overall survival; ROC, Receiver operating characteristic.

Comparison of Tumor Microenvironment, Immunotherapy, and TMB Between Groups

Based on the Wilcoxon test, high-risk ESCC patients showed considerably elevated immune, estimate, and stromal scores than low-risk patients (Figure 7A, $p < 0.05$). According to the findings in Figure 7B and C, there was a higher prevalence of M2 macrophages in high-risk ESCC patients, whereas the low-risk ESCC patients showed a higher prevalence of memory B cells, plasma cells, and monocytes. Upon comparison of the immune functions (Figure 7D), high-risk ESCC patients exhibited greater enrichment in co-inhibition of antigen-presenting cells (APCs), type I interferon response, and secondary inflammation in comparison to low-risk ESCC patients.

Analysis of the GSE53625 set revealed a positive correlation between risk score and TIDE (Figure 7E, R = 0.16, $p = 0.031$). Nonetheless, the disparity in TIDE between different risk groups did not achieve a level of statistical significance ($p = 0.051$). Although no statistically differences were found in TIDE between groups, low-risk ESCC patients had a 42% higher response rate to immunotherapy than high-risk ESCC patients (32%). A correlation between the TIDE and risk score was identified in the GSE53624 set (Figure 7F, R = 0.23, $p = 0.011$). Higher TIDE was found in high-risk ESCC patients ($p = 0.031$), while low-risk ESCC patients were predicted to respond to immunotherapy at a greater rate ($p = 0.027$).

https://doi.org/10.2147/OTT.S519270

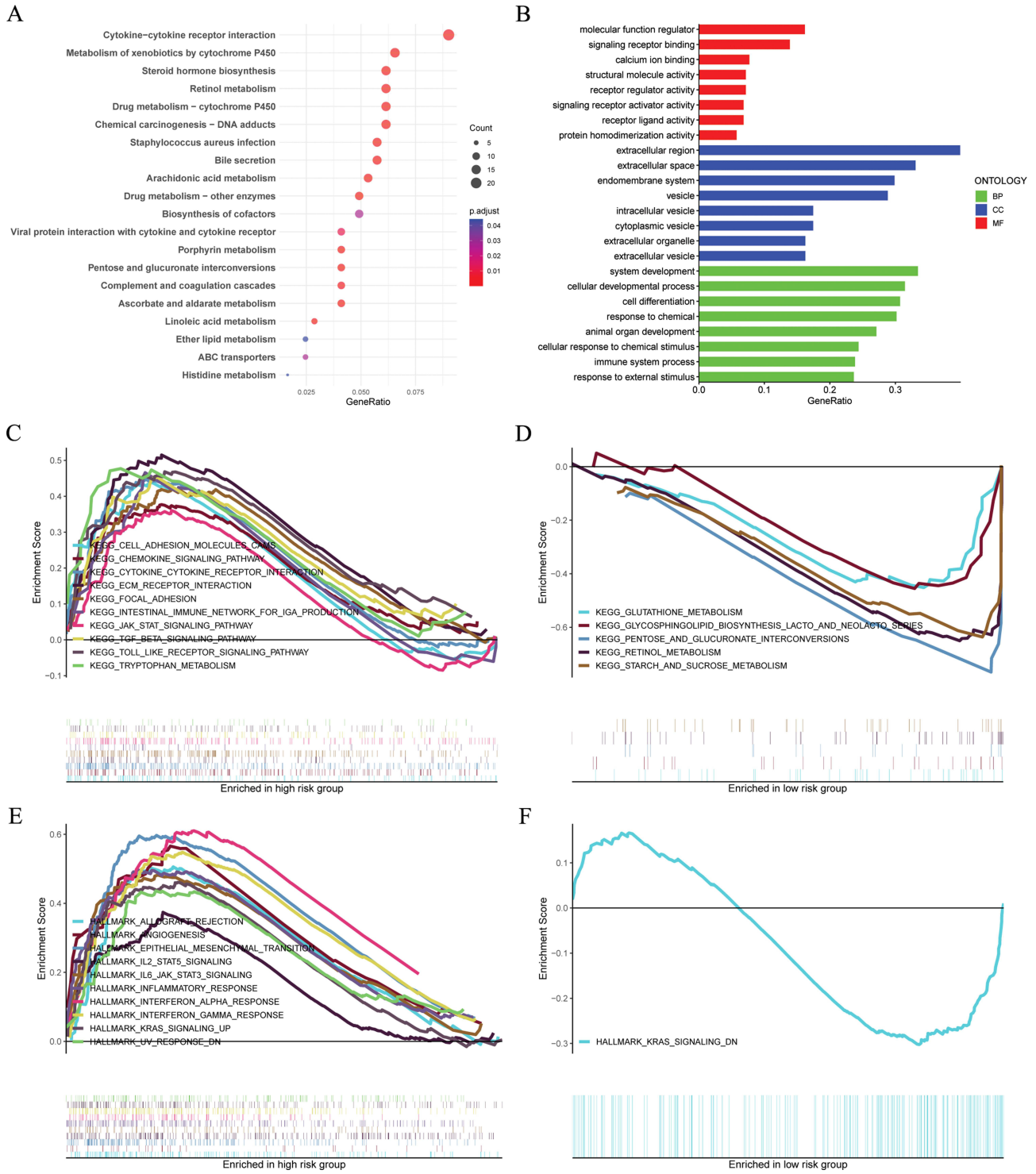

Figure 6 Functional enrichment analyses. (**A** and **B**) KEGG and GO enrichment analyses revealing the potential pathways enriched by the DEGs between the high- and low-risk groups. (**C**) GSEA analysis of different KEGG pathways focused on high-risk groups. (**D**) GSEA analysis of different KEGG pathways focused on low-risk groups. (**E**) GSEA analysis of different Hallmark pathways focused on high-risk groups. (**F**) GSEA analysis of different Hallmark pathways focused on low-risk groups.
Abbreviations: DEGs, different expression genes; KEGG, Kyoto Encyclopedia of Genes and Genomes; GO, Gene Ontology; GSEA, Gene Set Enrichment Analysis.

Subsequently, to assess whether risk scores and TMB are related, an analysis was conducted in TCGA-ESCC patients. The findings observed a negative correlation between TMB and risk score (Figure 7G, R = −0.23, p = 0.036). No statistically difference in TMB were observed between groups (Figure 7H, p = 0.22).

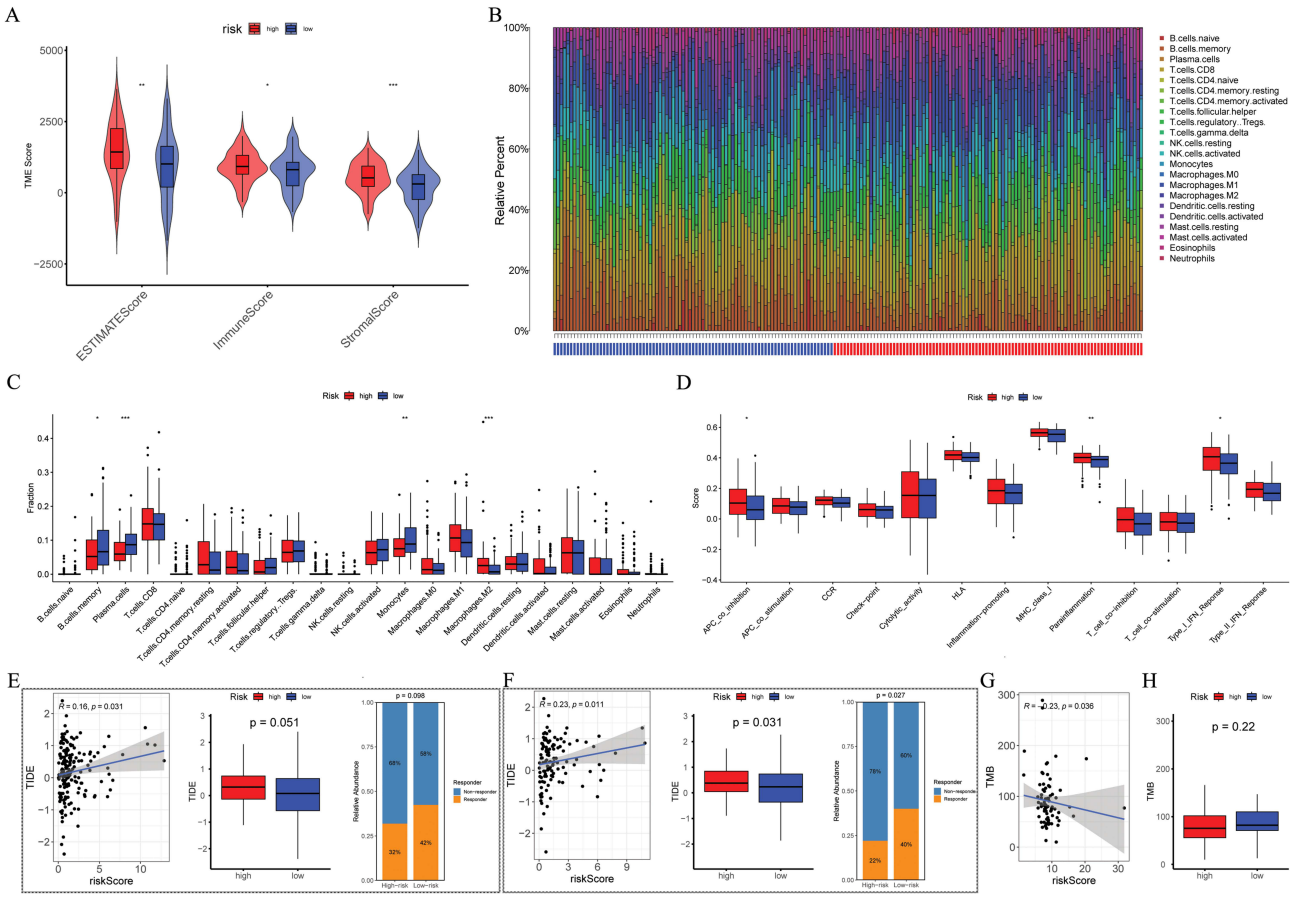

Figure 7 Immune infiltration analysis, and evaluation of immunotherapy response and TMB. (**A**) The ESTIMATE, Immune, Stromal Score were applied to quantify the different immune statuses between risk groups. (**B** and **C**) The CIBERSORT method was used to evaluate differences in the abundances of 22 types of immune cells between risk groups. (**D**) The ssGSEA algorithm was used to analyze differences in immune functions between risk groups. (**E**) In GSE53625 set, the correlation between risk score and TIDE, as well as TIDE expression and proportion of immunotherapy response in high-risk and low-risk groups. (**F**) In GSE53624 set, the correlation between risk score and TIDE, as well as TIDE expression and proportion of immunotherapy response in different risk groups. (**G** and **H**) In TCGA-ESCC set, the correlation between risk score and TMB, as well as TMB expression in different risk groups.

Notes: *$p < 0.05$, **$p < 0.01$, ***$p < 0.001$.

Abbreviations: ESCC, esophageal squamous cell carcinoma; ssGSEA, single sample gene set enrichment analysis; TIDE, tumor immune dysfunction and exclusion.TMB, tumor mutational burden.

Drug Sensitivity Analysis

Via Pearson correlation analysis, six compounds exhibiting the most significant correlation between IC50 values and risk scores were screened out. High-risk ESCC exhibited a greater sensitivity to erlotinib, acetalax, gefitinib, lapatinib, sapitinib, and afatinib (Figure 8A–F). The findings of the Wilcoxon test indicated that there were statistically significant differences in the IC50 values of the above six compounds between high - and low- risk ESCC patients ($p < 0.05$).

Validation of lncRNA Prognostic Signatures

We used qRT-PCR to validate the expression levels of six prognostic disulfidptosis-related lncRNAs in ESCC cells, comparing them to healthy Het-1A esophageal cells. The results indicated that AL359706.1 (Figure 9A) and AC011840.1 (Figure 9C) were significantly increased in ESCC cells, while the expression of four lncRNAs (AC025774.1, AC021683.3, AL121904.1, and AC079768.3) exhibited an opposite trend (Figure 9B, D–F).

Discussion

ESCC is a common cancer that leads to significant morbidity and mortality. Currently, the primary treatments for ESCC include both local and systemic approaches (endoscopic and surgical resection, neoadjuvant chemoradiotherapy,

https://doi.org/10.2147/OTT.S519270

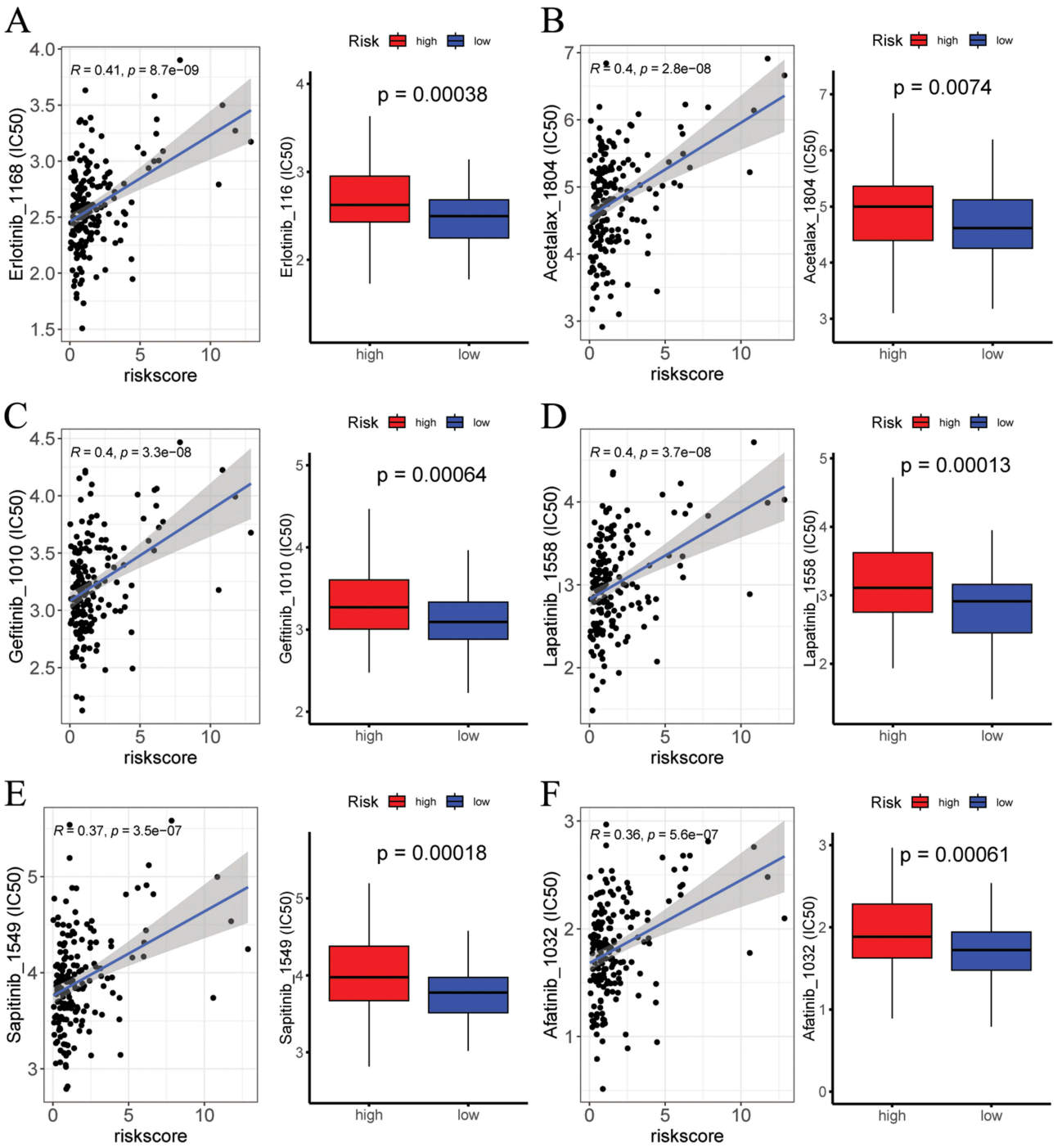

Figure 8 Correlation between risk score and drug sensitivity (IC50), and analysis of drug sensitivity (IC50) between risk groups. In the GSE53625 set (n = 179), (**A–F**) correlation scatter plot of IC50 of the top 6 candidate drugs (Erlotinib_1168, Acetalax_1804, Gefitinib_1010, Lapatinib_1558, Sapitinib_1549, and Afatinib_1032) and risk score, and boxplots of the difference in IC50 of candidate drugs between high- and low-risk groups. IC50, the half-maximal inhibitory concentration.

perioperative chemotherapy, and neoadjuvant chemotherapy).[5,45] However, due to its insidious pathogenesis and the fact that ESCC is a complex and highly heterogeneous tumor, the prognosis of ESCC patients remains unfavorable.[6–8] Liu et al recently reported disulfidptosis, potentially providing new anti-tumor therapy strategies.[9] Additionally, recently studies have suggested that lncRNAs play a role in regulating tumor development and tumorigenesis,[46] including in ESCC.[21,47] Numerous research investigations have substantiated the application of DRLs signature across diverse tumors, indicating its substantial prognostic and clinical significance. For instance, in laryngeal squamous cell

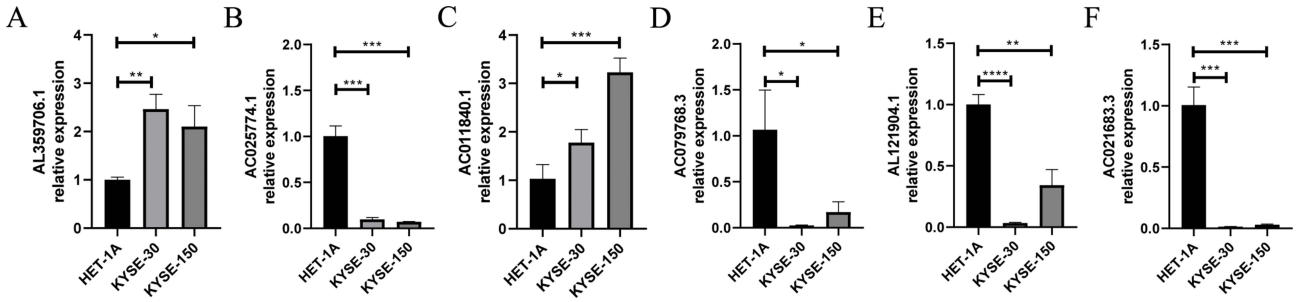

Figure 9 Exploration of the expression of 6 lncRNAs in healthy esophageal cells (Het-1A) and ESCC cells (KYSE-30 and KYSE-150). (**A**) AL359706.1. (**B**) AC025774.1. (**C**) AC011840.1. (**D**) AC079768.3. (**E**) AL121904.1. (**F**) AC021683.3.
Notes: $^{**}p < 0.05$, $^{**}p < 0.01$, $^{***}p < 0.001$, $^{****}p < 0.0001$.
Abbreviation: ESCC, esophageal squamous cell carcinoma.

carcinoma, Zhang et al[31] devised a DRLs signature discovered that this signature was outperformed traditional clinicopathological features in prognostic assessment. Moreover, in lung squamous cell carcinoma, Zhu et al[48] established a DRLs signature and demonstrated its crucial role in prognostic prediction, TME, and immunotherapy responses. However, the impact of DRLs signature on ESCC has not been fully elucidated. Thus, this research aimed to construct a DRLs prognostic signature for predicting ESCC prognosis and evaluating immunotherapy response effectiveness, ultimately seeking to improve OS in ESCC.

In this study, correlation analysis identified 3933 lncRNAs associated with disulfidptosis. Univariate Cox regression analysis of the training set identified 23 prognosis-related lncRNAs. Subsequently, LASSO and a multiple Cox regression analysis identified six prognostic DRLs—AL359706.1, AC025774.1, AC011840.1, AC021683.3, AC079768.3, and AL121904.1—and constructed a DRL signature. In terms of OS, low-risk ESCC patients showed notably better than high-risk ESCC patients. This finding was confirmed in the testing, GSE53625, GSE53624, and TCGA-ESCC sets. Besides, AUC curve of ESCC patients in the GSE53625 set validated the high predictive capacity of the 6-DRLs signatures, which were also verified in two external validation sets. Furthermore, the signature was suggested to be an independent prognostic factor for ESCC. A nomogram integrating clinical information with the 6-DRLs signatures demonstrated robust predictive performance, as the predicted OS closely matched the actual OS.

We examined the changes in functional enrichment of potential pathways for signaling, biological functional, and TME between groups to explore potential biological mechanisms. GSEA analysis indicated a notable distinction. Besides, individuals in high-risk had higher estimates, stromal, and immune scores, indicating more immune cell infiltration. Furthermore, M2 macrophages were significantly increased in groups at high, where B cell memory, plasma cells, and monocytes were significantly increased in groups at low. M2 macrophages, known to suppress inflammatory responses in solid tumors such as ESCC, are linked to poor clinical prognosis.[49–52] Clinical prognosis may be adversely affected by the accumulation of M2 macrophages, where the accumulation of B cell memory and plasma cells is associated with favorable clinical outcome.[53–55] The observed difference in prognosis between risk groups could potentially be explained by these findings.

Furthermore, we analyzed two groups on the basis of immune escape and immune therapy to investigate the predictive ability of DRLs signature for immune therapy sensitivity. The findings suggested lower TIDE scores observed in the low -risk ESCC group, indicating that individuals with low-risk ESCC may have an enhanced potential for responding positively to immunotherapy, whereas high-risk individuals are prone to immune evasion. Given the crucial role of TMB in determining tumors' response to immunotherapy, increased TMB levels could enhance the effectiveness of Immune Checkpoint Inhibitors.[34,56–58] The findings indicated an inverse correlation between TMB and risk score, with low-risk individuals showing higher TMB levels than high-risk individuals. This indicated a potential enhanced responsiveness to immunotherapy in low-risk individuals, aligning with the outcomes of TIDE. In addition to immunotherapy, the role of chemotherapy in antitumor therapy cannot be overstated. We examined the responses of individuals at varying risk levels to antitumor agents. These findings may offer some guidance for the selection of antitumor therapies in ESCC.

https://doi.org/10.2147/OTT.S519270

While this study presents novel and promising findings, there are several limitations. Firstly, we only conducted a few experiments to detect the expression of lncRNAs associated with disulfidptosis. Further exploration of the mechanisms of relevant lncRNAs in disulfidptosis will be the main focus of our future research. Secondly, given that our research relied heavily on bioinformatics and public databases for analyses, it is crucial to recognize the potential bias stemming from the relatively small sample size. Therefore, in the future, a larger sample of data is needed to further validate the predictive significance of DRLs signature in ESCC.

Conclusions

In this investigation, a robust predictive model, denoted as the DRLs signature, was established via bioinformatics methodologies. Our study is anticipated to enhance understanding of the expression patterns and roles of DRLs in ESCC, potentially improving the prognosis of ESCC patients. However, this study is retrospective and relies on public databases, with a limited sample size within the datasets. Moving forward, it is essential to conduct more extensive validation of the prognostic value and efficacy in real ESCC cohorts.

Data Sharing Statement

The original contributions presented in the study are included in the article, and further inquiries can be directed to the corresponding author.

Ethics Approval and Consent to Participate

The study was approved by The Medical Ethics Committee of the Sixth Affiliated Hospital of Nantong University with number 2024-135.

Acknowledgments

Special thanks go out to patients and researchers participating in TCGA and GEO for providing data for the authors.

Author Contributions

All authors made a significant contribution to the work reported, whether that is in the conception, study design, execution, acquisition of data, analysis and interpretation, or in all these areas; took part in drafting, revising or critically reviewing the article; gave final approval of the version to be published; have agreed on the journal to which the article has been submitted; and agree to be accountable for all aspects of the work.

Funding

This work was supported by Yancheng Medical Technology Development Program (YK2021008), Yancheng Key Research and Development Program (Social Development) (YCBE202324), the Medical Research Project of Yancheng Municipal Health Commission (YK2023021), the College-local collaborative innovation research project of Jiangsu Vocational College of medicine (202490110), and the Special Fundings for Science Development of the Clinical Teaching Hospitals of Jiangsu Vocational College of medicine (20229121 and 20219127).

Disclosure

The authors declare no conflicts of interest.

References

1. Morgan E, Soerjomataram I, Rumgay H, et al. The global landscape of esophageal squamous cell carcinoma and esophageal adenocarcinoma incidence and mortality in 2020 and projections to 2040: new estimates from GLOBOCAN 2020. *Gastroenterology*. 2022;163(3):649–658.e2. doi:10.1053/j.gastro.2022.05.054
2. Bray FF, Ferlay J, Soerjomataram I, Siegel RL, Torre LA, Jemal AJ. Erratum: global cancer statistics 2018: GLOBOCAN estimates of incidence and mortality worldwide for 36 cancers in 185 countries. *CA Cancer J Clin*. 2020;70(4):313. doi:10.3322/caac.21609
3. Chen W, Li H, Ren J, et al. Selection of high-risk individuals for esophageal cancer screening: a prediction model of esophageal squamous cell carcinoma based on a multicenter screening cohort in rural China. *Int, J, Cancer*. 2021;148(2):329–339. doi:10.1002/ijc.33208

4. Wu HX, Pan Y-Q, He Y, et al. Clinical benefit of first-line programmed death-1 antibody plus chemotherapy in low programmed cell death ligand 1-expressing esophageal squamous cell carcinoma: a post hoc analysis of JUPITER-06 and meta-analysis. *J Clin Oncol*. 2023;41(9):1735–1746. doi:10.1200/JCO.22.01490
5. Yan Y, Feng X, Li C, et al. Treatments for resectable esophageal cancer: from traditional systemic therapy to immunotherapy. *Chin Med J*. 2022;135(18):2143–2156. doi:10.1097/CM9.0000000000002371
6. Yang H, Li X, Yang W. Advances in targeted therapy and immunotherapy for esophageal cancer. *Chin Med J*. 2023;136(16):1910–1922. doi:10.1097/CM9.0000000000002768
7. Puhr HC, Prager GW, Ilhan-Mutlu A. How we treat esophageal squamous cell carcinoma. *ESMO Open*. 2023;8(1):100789. doi:10.1016/j.esmoop.2023.100789
8. Kakeji Y, Oshikiri T, Takiguchi G, et al. Multimodality approaches to control esophageal cancer: development of chemoradiotherapy, chemotherapy, and immunotherapy. *Esophagus*. 2021;18(1):25–32. doi:10.1007/s10388-020-00782-1
9. Liu X, Nie L, Zhang Y, et al. Actin cytoskeleton vulnerability to disulfide stress mediates disulfidptosis. *Nat Cell Biol*. 2023;25(3):404–414. doi:10.1038/s41556-023-01091-2
10. Zheng P, Zhou C, Ding Y, et al. Disulfidptosis: a new target for metabolic cancer therapy. *J Exp Clin Cancer Res*. 2023;42(1):103. doi:10.1186/s13046-023-02675-4
11. Yang L, Liu J, Li S, et al. Based on disulfidptosis, revealing the prognostic and immunological characteristics of renal cell carcinoma with tumor thrombus of vena cava and identifying potential therapeutic target AJAP1. *J Cancer Res Clin Oncol*. 2023;149(12):9787–9804. doi:10.1007/s00432-023-04877-x
12. Zhao S, Wang L, Ding W, et al. Crosstalk of disulfidptosis-related subtypes, establishment of a prognostic signature and immune infiltration characteristics in bladder cancer based on a machine learning survival framework. *Front Endocrinol*. 2023;14:1180404. doi:10.3389/fendo.2023.1180404
13. Wang T, Guo K, Zhang D, et al. Disulfidptosis classification of hepatocellular carcinoma reveals correlation with clinical prognosis and immune profile. *Int Immunopharmacol*. 2023;120:110368. doi:10.1016/j.intimp.2023.110368
14. Chen H, Yang W, Li Y, et al. Leveraging a disulfidptosis-based signature to improve the survival and drug sensitivity of bladder cancer patients. *Front Immunol*. 2023;14:1198878. doi:10.3389/fimmu.2023.1198878
15. Feng Z, Zhao Q, Ding Y, et al. Identification a unique disulfidptosis classification regarding prognosis and immune landscapes in thyroid carcinoma and providing therapeutic strategies. *J Cancer Res Clin Oncol*. 2023;149(13):11157–11170. doi:10.1007/s00432-023-05006-4
16. Xue W, Qiu K, Dong B, et al. Disulfidptosis-associated long non-coding RNA signature predicts the prognosis, tumor microenvironment, and immunotherapy and chemotherapy options in colon adenocarcinoma. *Cancer Cell Int*. 2023;23(1):218. doi:10.1186/s12935-023-03065-8
17. Liu Y, Meng J, Ruan X, et al. A disulfidptosis-related lncRNAs signature in hepatocellular carcinoma: prognostic prediction, tumor immune microenvironment and drug susceptibility. *Sci Rep*. 2024;14(1):746. doi:10.1038/s41598-024-51459-z
18. Xu L, Chen S, Li Q, et al. Integrating bioinformatics and experimental validation to unveil disulfidptosis-related lncRNAs as prognostic biomarker and therapeutic target in hepatocellular carcinoma. *Cancer Cell Int*. 2024;24(1):30. doi:10.1186/s12935-023-03208-x
19. Yao H, Liu P, Yao L, et al. Establishment of disulfidptosis-related LncRNA signature as biomarkers in colon adenocarcinoma. *Cancer Cell Int*. 2024;24(1):183. doi:10.1186/s12935-024-03374-6
20. Ye Y, Ge O, Zang C, et al. LINC01094 predicts poor prognosis in patients with gastric cancer and is correlated with EMT and macrophage infiltration. *Technol Cancer Res Treat*. 2022;21:15330338221080977. doi:10.1177/15330338221080977
21. Zhou M, Bao S, Gong T, et al. The transcriptional landscape and diagnostic potential of long non-coding RNAs in esophageal squamous cell carcinoma. *Nat Commun*. 2023;14(1):3799. doi:10.1038/s41467-023-39530-1
22. Huang T, You Q, Huang D, et al. A positive feedback between PDIA3P1 and OCT4 promotes the cancer stem cell properties of esophageal squamous cell carcinoma. *Cell Commun Signal*. 2024;22(1):60. doi:10.1186/s12964-024-01475-3
23. Zhao L, Wang G, Qi H, et al. LINC00330/CCL2 axis-mediated ESCC TAM reprogramming affects tumor progression. *Cell Mol Biol Lett*. 2024;29(1):77. doi:10.1186/s11658-024-00592-8
24. Xue ST, Cao S-Q, Ding J-C, et al. LncRNA LUESCC promotes esophageal squamous cell carcinoma by targeting the miR-6785-5p/NRSN2 axis. *Cell Mol Life Sci*. 2024;81(1):121. doi:10.1007/s00018-024-05172-9
25. Zhang X, Feng N, Wu B, et al. Prognostic value and immune landscapes of cuproptosis-related lncRNAs in esophageal squamous cell carcinoma. *Aging*. 2023;15(19):10473–10500. doi:10.18632/aging.205089
26. Zheng X, Liu W, Zhu Y, et al. Development and validation of the oxidative stress related lncRNAs for prognosis in esophageal squamous cell carcinoma. *Cancers*. 2023;15(17):4399. doi:10.3390/cancers15174399
27. Han L, Yang H, Jiang X, et al. Prognostic model based on disulfidptosis-related lncRNAs for predicting survival and therapeutic response in bladder cancer. *Front Immunol*. 2024;15:1512203. doi:10.3389/fimmu.2024.1512203
28. Hu XC, Yu Q-Y, Ding H-P, et al. Exploration on the construction of a bladder cancer prognostic model based on disulfidptosis-related lncRNAs and its clinical significance. *Sci Rep*. 2024;14(1):26751. doi:10.1038/s41598-024-78481-5
29. Xiao J, Liu W, Gong J, et al. Integrated single-cell analysis reveals the regulatory network of disulfidptosis-related lncRNAs in bladder cancer: constructing a prognostic model and predicting treatment response. *Front Oncol*. 2025;15:1527036. doi:10.3389/fonc.2025.1527036
30. Mulati Y, Lai C, Luo J, et al. Establishment of a prognostic risk prediction model incorporating disulfidptosis-related lncRNA for patients with prostate cancer. *BMC Cancer*. 2024;24(1):44. doi:10.1186/s12885-023-11778-2
31. Zhang M, Sun Q, Han Z, et al. Construction of a novel disulfidptosis-related lncRNAs signature for prognosis prediction and anti-tumor immunity in laryngeal squamous cell carcinoma. *Heliyon*. 2024;10(10):e30877. doi:10.1016/j.heliyon.2024.e30877
32. Hong S, Zhang Y, Wang D, et al. Disulfidptosis-related lncRNAs signature predicting prognosis and immunotherapy effect in lung adenocarcinoma. *Aging*. 2024;16(11):9972–9989. doi:10.18632/aging.205911
33. Liu S, Wang S, Guo J, et al. Crosstalk among disulfidptosis-related lncRNAs in lung adenocarcinoma reveals a correlation with immune profile and clinical prognosis. *Noncoding RNA Res*. 2024;9(3):772–781. doi:10.1016/j.ncrna.2024.03.006
34. Song Z, Cao X, Wang X, et al. A disulfidptosis-related lncRNA signature for predicting prognosis and evaluating the tumor immune microenvironment of lung adenocarcinoma. *Sci Rep*. 2024;14(1):4621. doi:10.1038/s41598-024-55201-7

35. Guo Z, Xie Y, Zhang L, et al. A novel disulfidptosis-related lncRNAs signature for predicting survival and immune response in hepatocellular carcinoma. *Aging*. 2024;16(1):267–284. doi:10.18632/aging.205367
36. Pu L, Sun Y, Pu C, et al. Machine learning-based disulfidptosis-related lncRNA signature predicts prognosis, immune infiltration and drug sensitivity in hepatocellular carcinoma. *Sci Rep*. 2024;14(1):4354. doi:10.1038/s41598-024-54115-8
37. Blanche P, Dartigues JF, Jacqmin-Gadda H. Estimating and comparing time-dependent areas under receiver operating characteristic curves for censored event times with competing risks. *Stat Med*. 2013;32(30):5381–5397. doi:10.1002/sim.5958
38. Zhang Z, Kattan MW. Drawing Nomograms with R: applications to categorical outcome and survival data. *Ann Transl Med*. 2017;5(10):211. doi:10.21037/atm.2017.04.01
39. Ritchie ME, Phipson B, Wu D, et al. limma powers differential expression analyses for RNA-sequencing and microarray studies. *Nucleic Acids Res*. 2015;43(7):e47. doi:10.1093/nar/gkv007
40. Yu G, Wang L-G, Han Y, et al. clusterProfiler: an R package for comparing biological themes among gene clusters. *Omics*. 2012;16(5):284–287. doi:10.1089/omi.2011.0118
41. Newman AM, Liu CL, Green MR, et al. Robust enumeration of cell subsets from tissue expression profiles. *Nat Methods*. 2015;12(5):453–457. doi:10.1038/nmeth.3337
42. Jiang P, Gu S, Pan D, et al. Signatures of T cell dysfunction and exclusion predict cancer immunotherapy response. *Nat Med*. 2018;24 (10):1550–1558. doi:10.1038/s41591-018-0136-1
43. Mayakonda A, Lin D-C, Assenov Y, et al. Maftools: efficient and comprehensive analysis of somatic variants in cancer. *Genome Res*. 2018;28 (11):1747–1756. doi:10.1101/gr.239244.118
44. Maeser D, Gruener RF, Huang RS. oncoPredict: an R package for predicting in vivo or cancer patient drug response and biomarkers from cell line screening data. *Brief Bioinform*. 2021;22(6). doi:10.1093/bib/bbab260
45. Ajani JA, D'Amico TA, Bentrem DJ, et al. Esophageal and esophagogastric junction cancers, version 2.2019, NCCN clinical practice guidelines in oncology. *J Natl Compr Canc Netw*. 2019;17(7):855–883. doi:10.6004/jnccn.2019.0033
46. Ahmad M, Weiswald L-B, Poulain L, et al. Involvement of lncRNAs in cancer cells migration, invasion and metastasis: cytoskeleton and ECM crosstalk. *J Exp Clin Cancer Res*. 2023;42(1):173. doi:10.1186/s13046-023-02741-x
47. Xue ST, Zheng B, Cao S-Q, et al. Long non-coding RNA LINC00680 functions as a ceRNA to promote esophageal squamous cell carcinoma progression through the miR-423-5p/PAK6 axis. *Mol Cancer*. 2022;21(1):69. doi:10.1186/s12943-022-01539-3
48. Zhu A, Zong Y, Gao X. Development of a disulfidptosis-related lncRNA prognostic signature for enhanced prognostic assessment and therapeutic strategies in lung squamous cell carcinoma. *Sci Rep*. 2024;14(1):17804. doi:10.1038/s41598-024-68423-6
49. Zhao Y, Sun J, Li Y, et al. Tryptophan 2,3-dioxygenase 2 controls M2 macrophages polarization to promote esophageal squamous cell carcinoma progression via AKT/GSK3β/IL-8 signaling pathway. *Acta Pharm Sin B*. 2021;11(9):2835–2849. doi:10.1016/j.apsb.2021.03.009
50. Xu Y, Liao C, Liu R, et al. IRGM promotes glioma M2 macrophage polarization through p62/TRAF6/NF-κB pathway mediated IL-8 production. *Cell Biol Int*. 2019;43(2):125–135. doi:10.1002/cbin.11061
51. Xu Y, Cui G, Jiang Z, et al. Survival analysis with regard to PD-L1 and CD155 expression in human small cell lung cancer and a comparison with associated receptors. *Oncol Lett*. 2019;17(3):2960–2968. doi:10.3892/ol.2019.9910
52. Cassetta L, Pollard JW. Targeting macrophages: therapeutic approaches in cancer. *Nat Rev Drug Discov*. 2018;17(12):887–904. doi:10.1038/nrd.2018.169
53. Yao C, Yu H, Zhou G, et al. Tumor-infiltrating plasma cells are the promising prognosis marker for esophageal squamous cell carcinoma. *Esophagus*. 2021;18(3):574–584. doi:10.1007/s10388-021-00828-y
54. Fridman WH, Meylan M, Pupier G, et al. Tertiary lymphoid structures and B cells: an intratumoral immunity cycle. *Immunity*. 2023;56 (10):2254–2269. doi:10.1016/j.immuni.2023.08.009
55. Laumont CM, Banville AC, Gilardi M, et al. Tumour-infiltrating B cells: immunological mechanisms, clinical impact and therapeutic opportunities. *Nat Rev Cancer*. 2022;22(7):414–430. doi:10.1038/s41568-022-00466-1
56. Chan TA, Wolchok JD, Snyder A. Genetic basis for clinical response to CTLA-4 blockade in melanoma. *N Engl J Med*. 2015;373(20):1984. doi:10.1056/NEJMc1508163
57. Rizvi NA, Hellmann MD, Snyder A, et al. Mutational landscape determines sensitivity to PD-1 blockade in non-small cell lung cancer. *Science*. 2015;348(6230):124–128. doi:10.1126/science.aaa1348
58. Chen C, Wang C, Li Y, et al. Prognosis and chemotherapy drug sensitivity in liver hepatocellular carcinoma through a disulfidptosis-related lncRNA signature. *Sci Rep*. 2024;14(1):7157. doi:10.1038/s41598-024-57954-7